

INTRODUCTION

The Maryland Department of Business and Economic Development (DBED) has a mission to attract new companies to Maryland. DBED has chosen to target the Cyber Security business sector for growth within the state.

At DBED, Business Representatives are responsible for working directly with companies interested in locating in Maryland. This process is referred to as the site selection process. It is the responsibility of the Business Representatives to market Maryland as the best place to do business based on available resources and competitive investment opportunities.

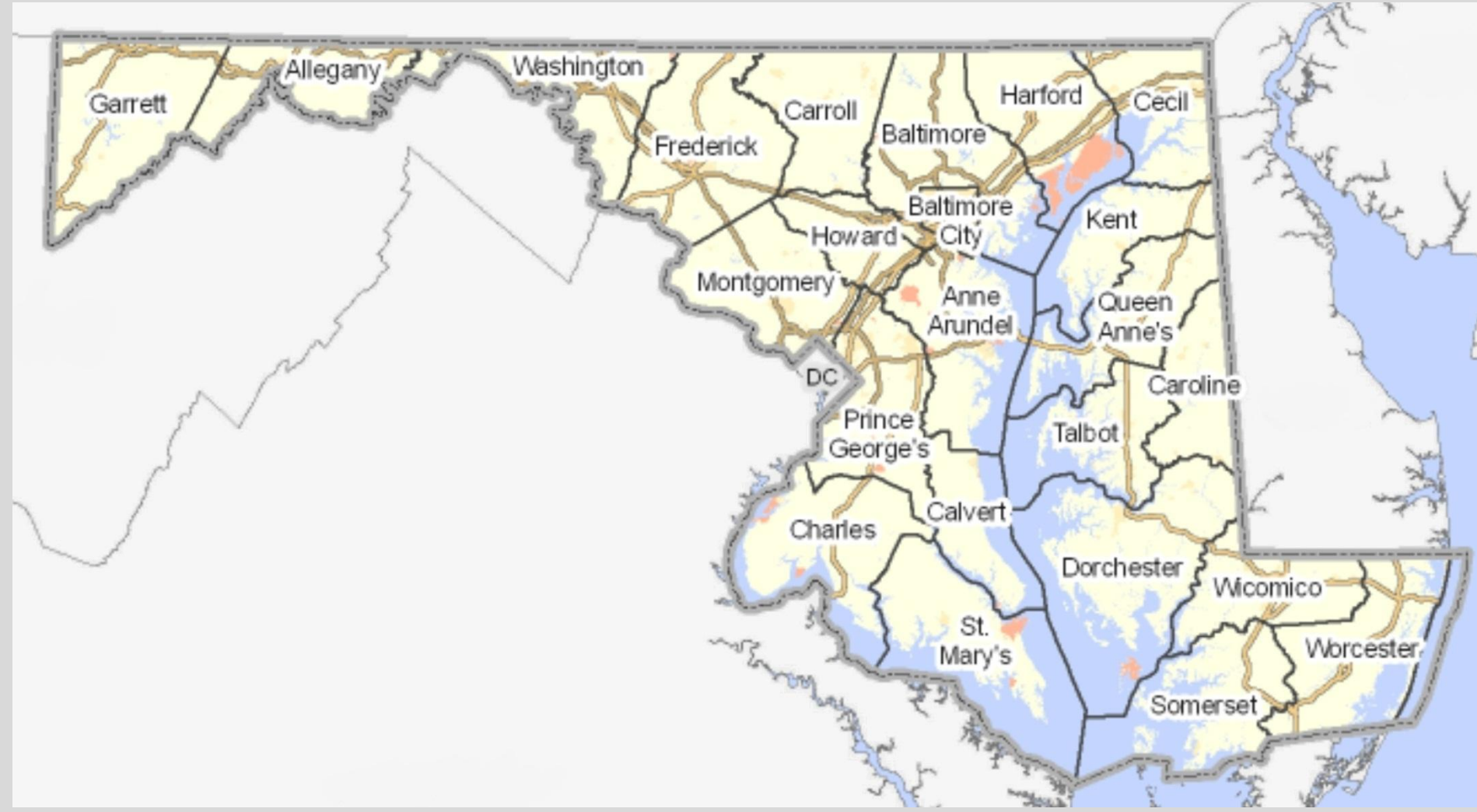
OBJECTIVES

This study introduces a new approach to the site selection process. A GIS-based suitability study will be conducted identifying and ranking areas of Maryland for a Cyber Security company to locate.

Available properties in these suitable areas will be identified and all results will be provided as a preliminary resource to Business Representatives working with Cyber Security companies looking to locate their company in Maryland.

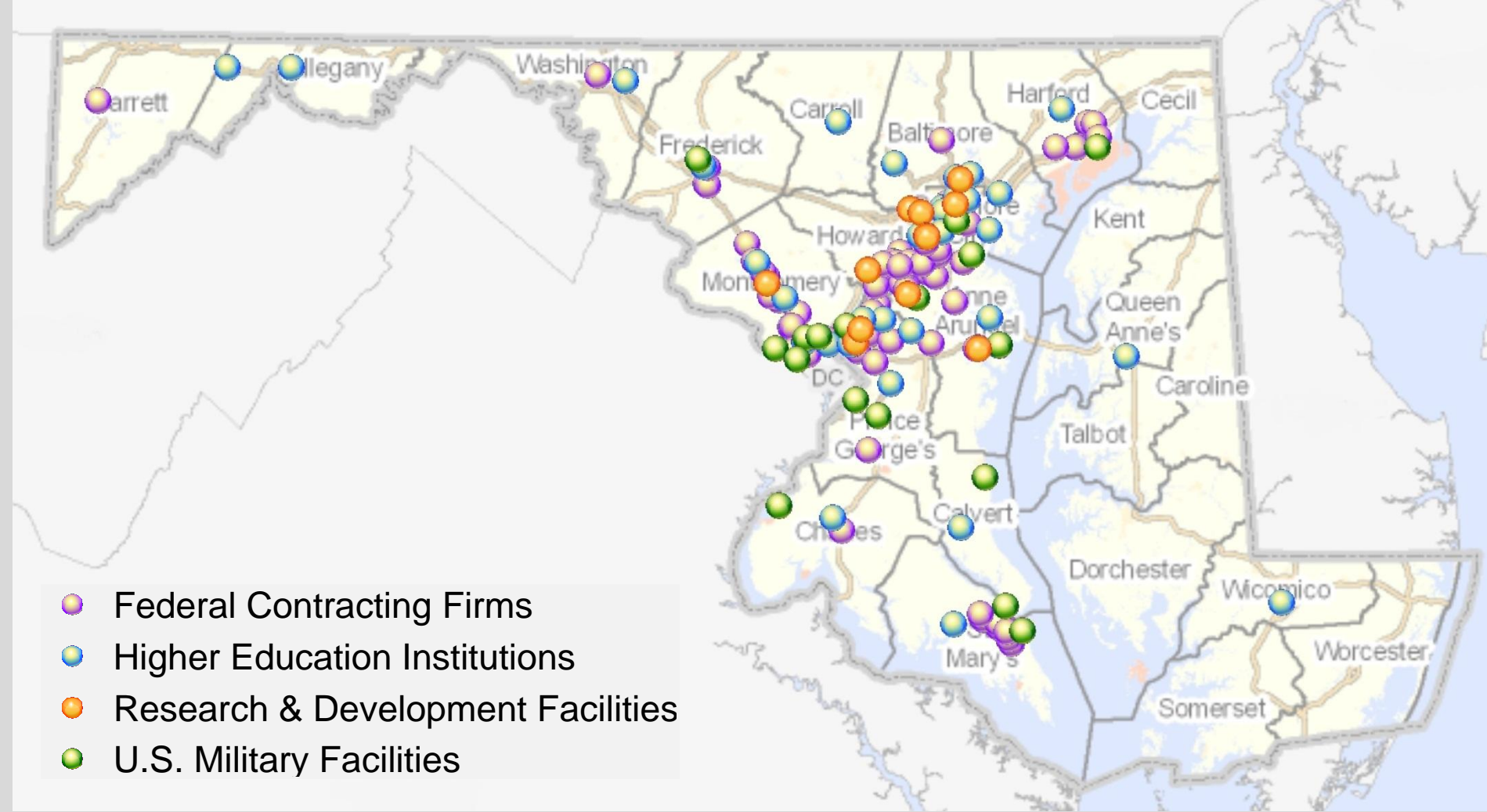
STUDY AREA

DBED is a state agency and is dedicated to attracting companies to all regions of the state. This study will be conducted for the entire state of Maryland.



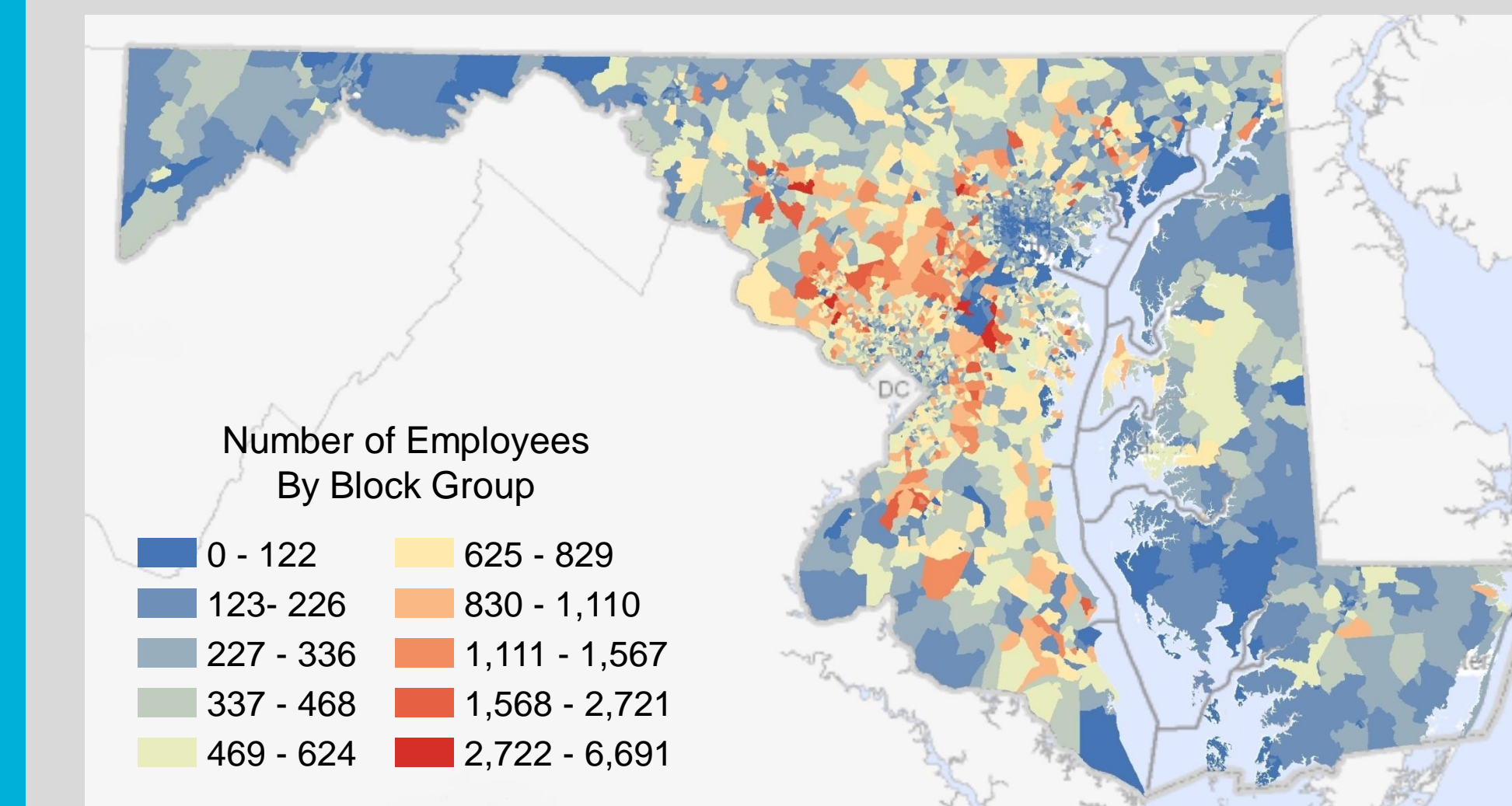
DATA

There are four main Cyber Security resources located across the entire state of Maryland.

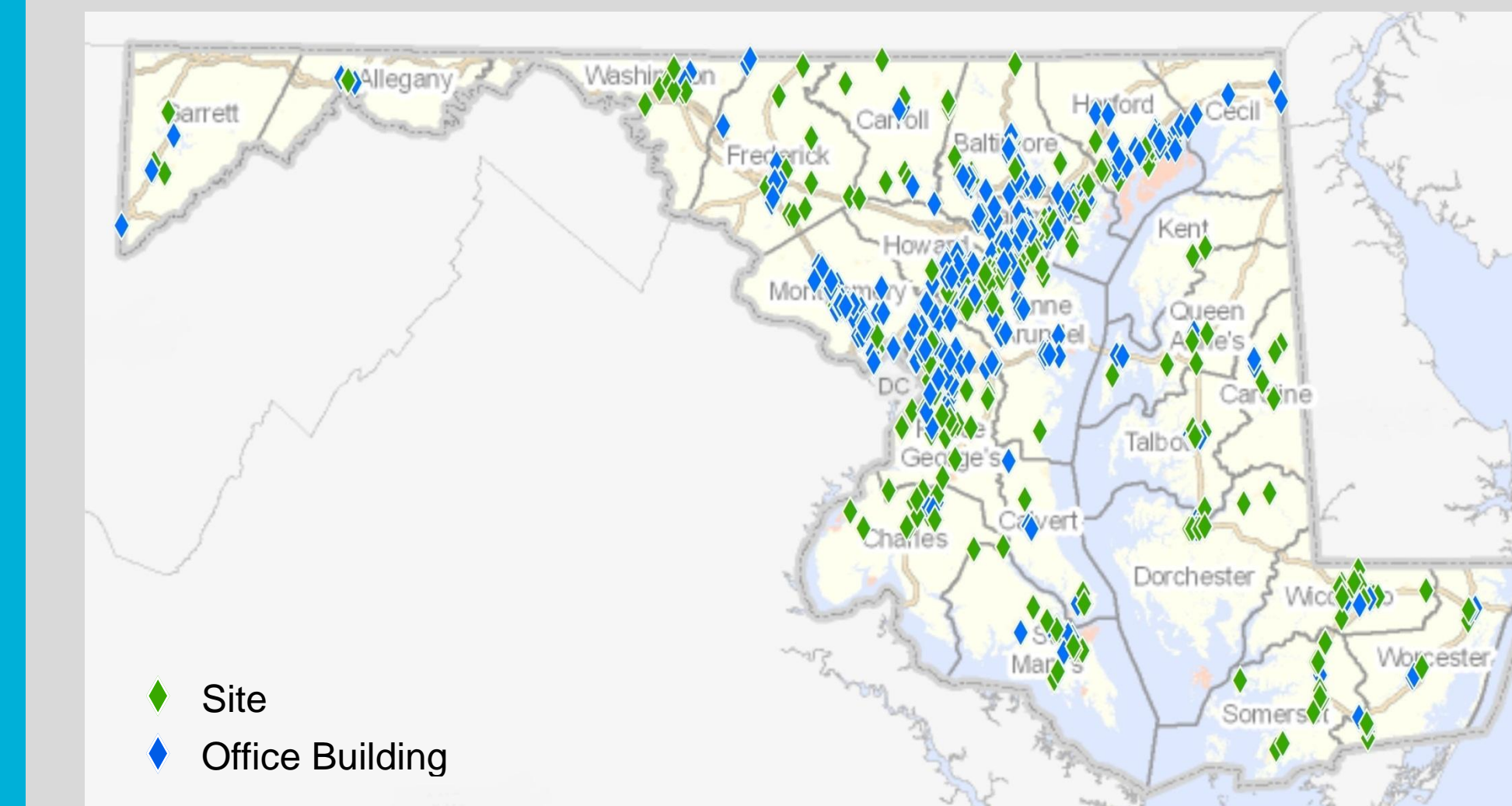


DATA CONTINUED...

Another resource is a highly skilled workforce which is represented as polygon-based demographic data for 2009.



Another resource is DBED's database of available properties for lease/sale located throughout Maryland.



METHODS

Step #1 – Data Conversion: The workforce polygon layer was converted into a raster based on percentage of desired workforce of the total population. The desired workforce includes those in Computer, Management and Engineering occupations.

Step #2 – Euclidean Distance Analysis: The Euclidean distance analysis was performed for the four main Cyber Security resources vector data layers at 5, 10, 15, 20, 25, 30, 35, 40 & 45 miles. It was assumed that after 45 miles, the relevance of distance dropped off significantly.

Step #3 – Reclassification of Rasters: All five resource rasters were reclassified and ranked 1 – 10 (1 = lowest ranking and 10 = highest ranking)

Step #4 – Weighted Raster Calculation: All five resource rasters were assigned a weight significance which were used in the raster calculation.

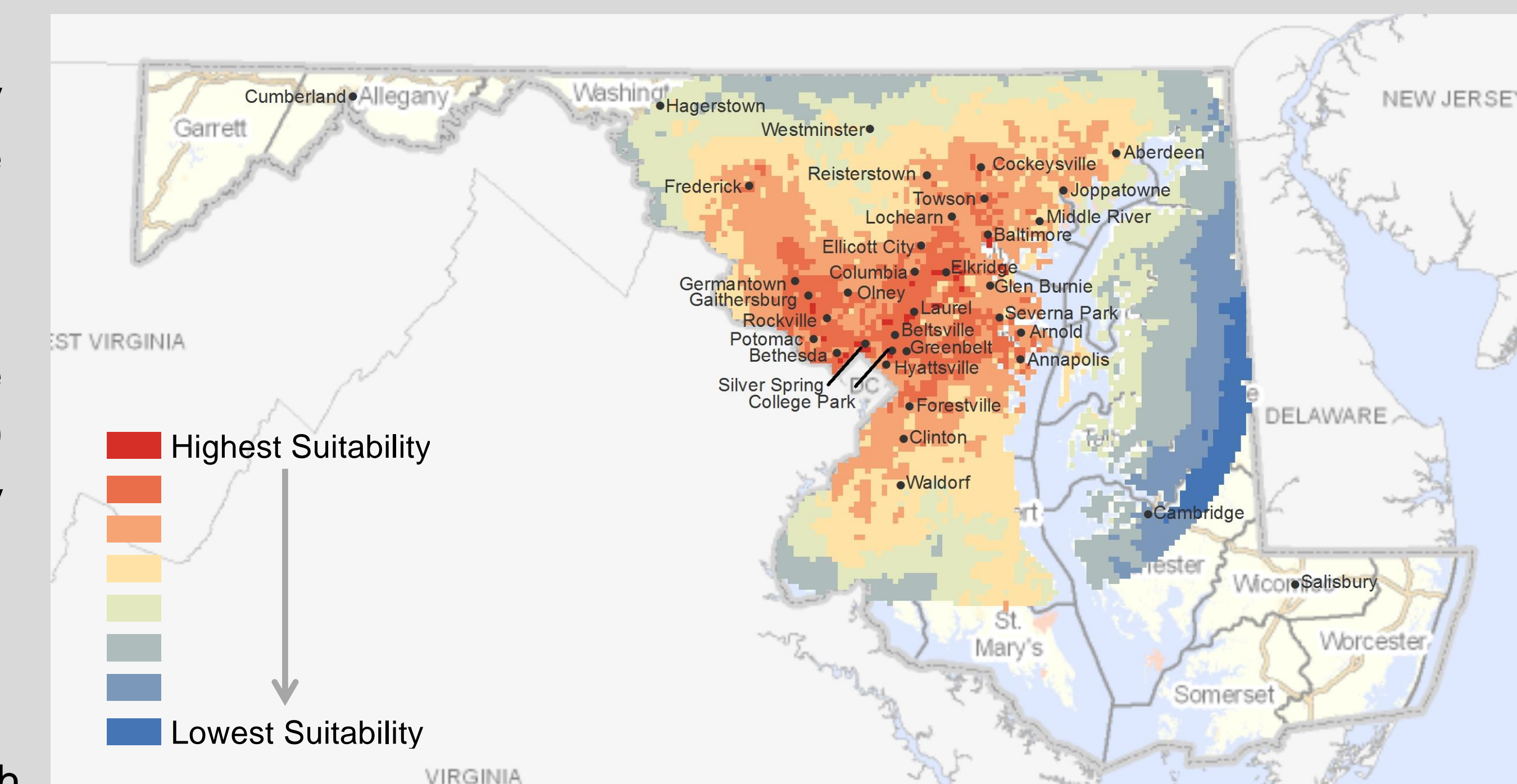
- Available Workforce = 25%
- Federal Contracting Firms = 20%
- Research & Development Facilities = 20%
- U.S. Military Facilities = 20%
- Higher Education Institutions = 15%

Step #5 – Available Properties Comparison: The results were compared with the available properties to identify properties for Cyber Security companies to locate within the suitable areas of Maryland.

RESULTS & DISCUSSION

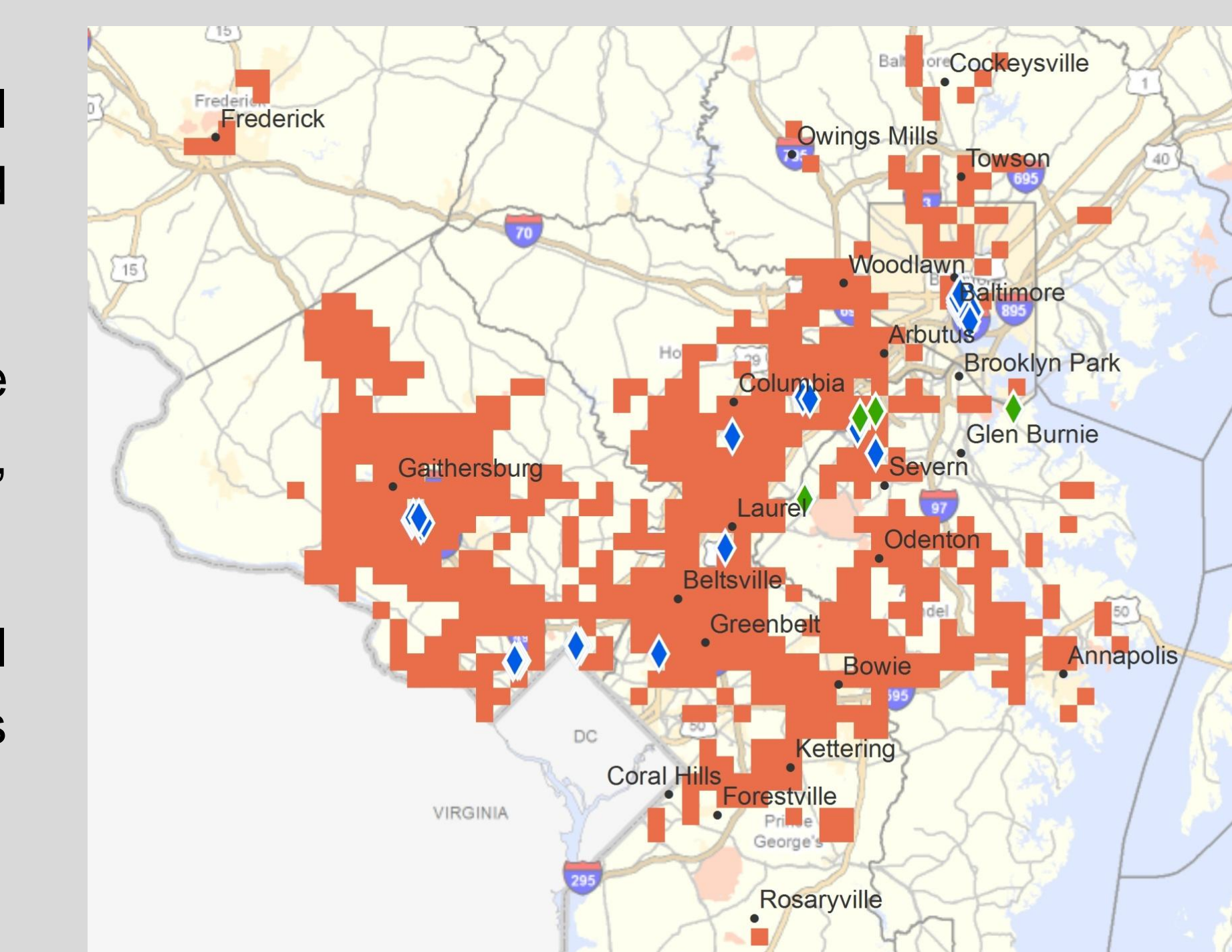
Highest Suitability:

The areas of highest suitability for a Cyber Security company are located in the central corridor of the state, including Baltimore, Bethesda, Laurel, Rockville and Silver Spring.



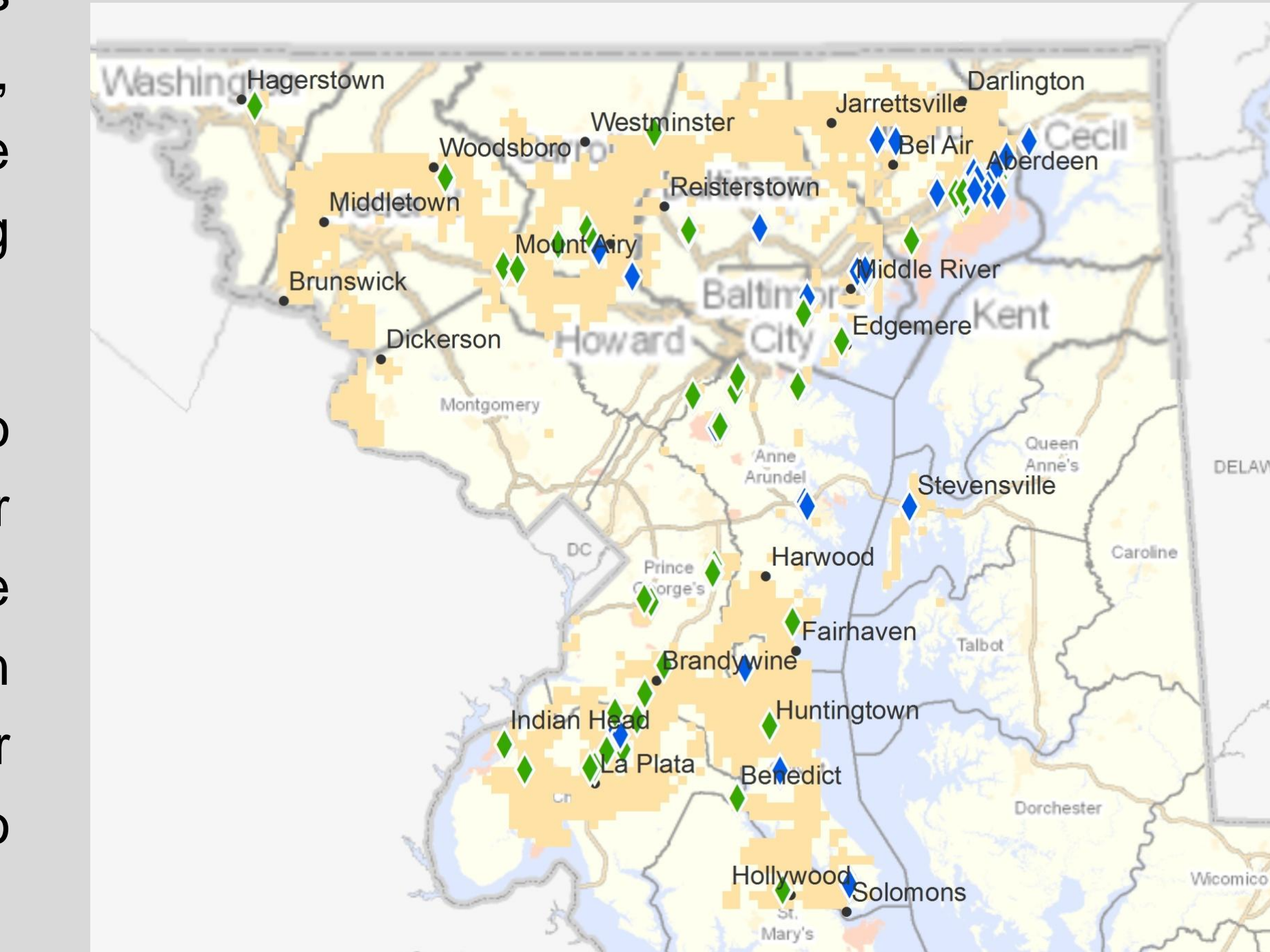
High Suitability:

This study has also revealed areas with high suitability outside of the central corridor of the state. These areas have available properties that would still be very close to all desired Cyber Security resources, but offer more competitive lease and sale prices.



There are 478 properties available in the high suitability areas. These properties are available in Annapolis, Beltsville, Capitol Heights, Frederick, Hanover, Linthicum, Timonium and White Marsh.

A more competitive lease/sale price location is a significant marketing tool when working with potential companies and is very valuable to Business Representatives in this highly competitive market.



Moderate Suitability:

Although at the outset, this suitability does not appear to be of interest, it is worth further investigation. Within this area of suitability is Hagerstown, which is an area that is known for a highly intelligent and productive workforce and has seen a number of significant company closures during the down economy.

This suitability area also reaches into St. Mary's County which is close to some very significant military facilities. Companies that have a higher interest in being within close proximity to a military facility rather than the other Cyber Security resources, may place properties in this area higher on their site selection list. Additional factors, which were not considered for this study, such as affordable housing and median income could also influence a companies' ultimate decision.

CONCLUSION

This project was designed to provide the Business Representatives at DBED with an additional tool to assist them with bringing Cyber Security companies to Maryland. The results of this study will support the marketing efforts of revealing Maryland as an excellent state to locate a Cyber Security company. Additionally, the methods of this study have been designed in such a way to allow for adjustments accommodating analysis of additional resources and factors and can also be adapted for analysis of other business sectors.

ACKNOWLEDGEMENT

Maryland Department of Business and Economic Development: www.choosemaryland.org

Esri: www.esri.com

MD iMap: mdimap.towson.edu/Portal or MD iMap Map Services: mdimap.towson.edu/arcgis/rest/services

Spatial Analysis of Corn Productivity in a Variable-Rate Nitrogen Plot

William A. White, USDA-ARS Hydrology & Remote Sensing Laboratory

Abstract

Nitrogen (N) fertilizer is applied to corn fields to supplement growth. However, runoff of excess N harms the surrounding environment. Multiple N treatments are compared using ArcGIS to analyze *in situ* measurements. Nitrogen stress is confirmed in no-treatment plots and higher productivity is seen in fertilized plots. The Red Edge Chlorophyll Index (RECI), is shown to be more effective than NDVI at predicting productivity remotely.

Introduction

Precision agriculture minimizes waste and environmental degradation by applying N in variable rates, based on plant stress. Remote sensing indices such as NDVI are commonly used for vegetation assessments. Another index called the Red Edge Chlorophyll Index (RECI) is linked specifically to chlorophyll content (Gitelson et al., 2006). RECI utilizes the 'red-edge', 690-740nm, which is positively related to chlorophyll content and may be the most relevant property in the prediction of productivity.

Study Area

The study was conducted in 2010 at the Beltsville Agricultural Research Center in Beltsville, Maryland for the Optimizing Production Inputs for Economic and Environmental Enhancement (OPE3) project. Corn was planted May 16 and N was applied June 1. The 6200-square-meter study area was split into 12 plots which received one of 4 N treatments: 0, 70, 140, and 280 kg N/hectare. (See Figure 1.) The plots each contained 3 sampling points which were used throughout the study.

Data & Methods

Field and airborne measurements were taken during plant growth (Figure 2). Plots were harvested by hand on Sept. 22 and yield was measured by weight.



Figure 2. *In situ* measurements: 1. Plant Height; 2. Leaf Chlorophyll (SPAD meter); 3. Spectral Reflectance (CropScan); 4. Leaf Area Index (LiCor LAI2000); 5. Aerial Hyperspectral Imagery (SpecTIR).

Field data from June 23, July 2, and July 17 were analyzed in ArcGIS.

- Data were joined to GPS points.
- NDVI and RECI were added as new entities and populated using Field Calculator, on CropSCAN canopy spectral reflectance (R) values.

$$NDVI = (R_{780} - R_{670}) / (R_{780} + R_{670})$$

$$RECI = (R_{780}/R_{720}) - 1$$

- Attribute tables were summarized by plot ID for mean, maximum, and minimum values. The locations of the highest and lowest plot means were recorded (Figure 3).
- Cluster and Outlier Analyses (Anselin Local Moran's I) were conducted.
- Scatter plot matrices were created for each date and coefficients of determination (r^2) were computed using Ordinary Least Squares (OLS) regression. (See Figure 4.)

Hyperspectral imagery from July 17 was analyzed in ArcGIS.

- An airborne sensor (SpecTIR) acquired 360 bands of VNIR/SWIR reflectance data. The 670nm, 720nm, and 780nm bands were loaded as separate rasters.
- Environment settings were modified to match the extent of the plot boundaries.
- Raster Calculator was used to create new rasters representing NDVI and RECI.
- Zonal Statistics were performed to locate the plots in which the highest/lowest averages, maximum, and minimum values occurred (Figure 3).

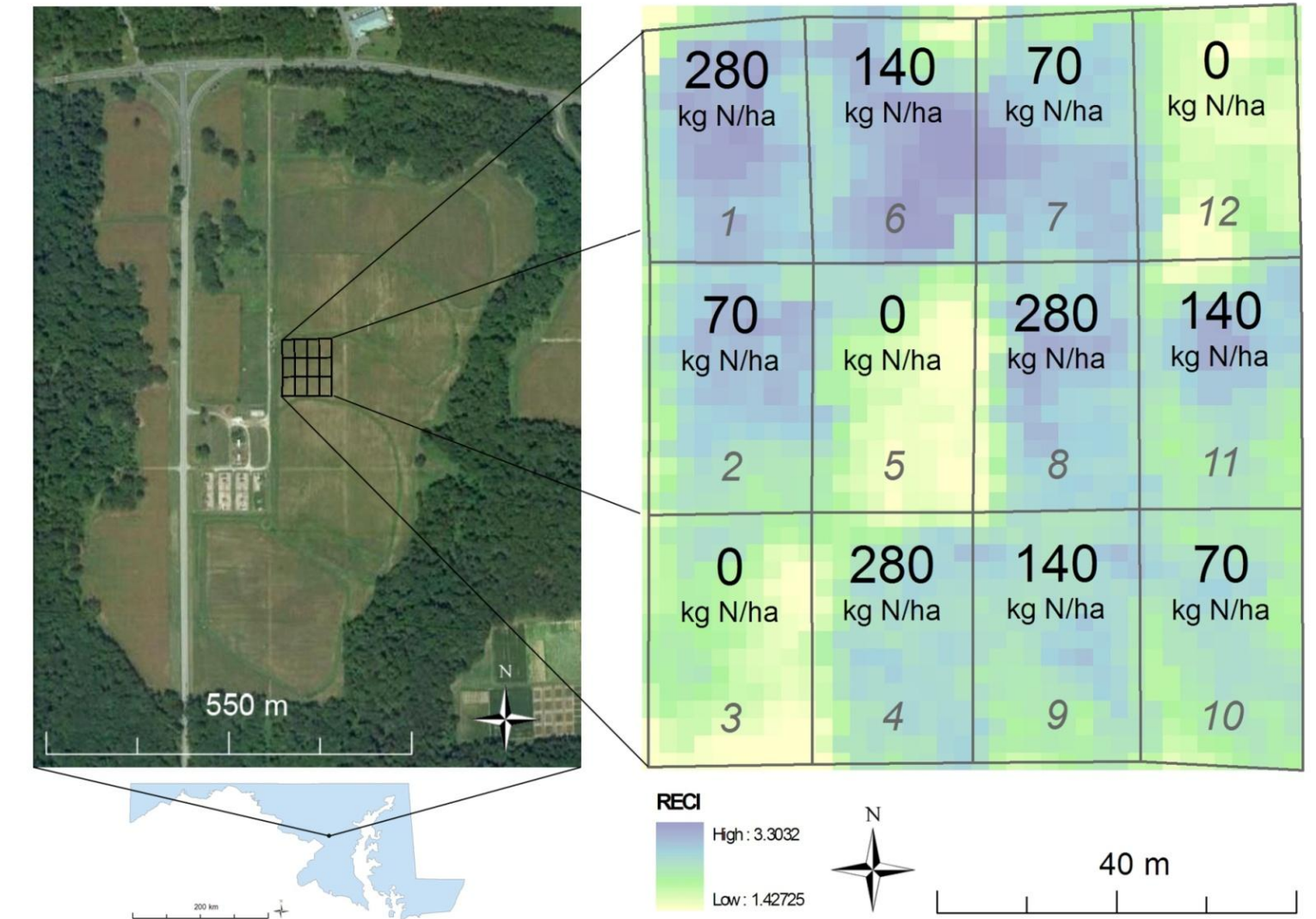


Figure 1. OPE3 study site in Beltsville, MD, August 2010 (left); Nitrogen plot showing RECI from hyperspectral imagery, July 2010 (right).

Results & Discussion

Data summaries (Figure 3) revealed that plots treated with 280 kg N/ha contained the healthiest plants at all growth stages examined. Untreated plots contained the least-healthy plants. This trend was most prevalent as plants reached full height and began to tassel around July 17. Notable exceptions occurred in the hyperspectral data and may be due to within-plot variability overlooked by field sampling (3 points per plot). Atmospheric interference may also have played a role as some clouds were present on the day of imagery acquisition.

	June 23, 2010											
	Highest Mean			Lowest Mean			Max			Min		
	Plot#	N	Value	Plot#	N	Value	Plot#	N	Value	Plot#	N	Value
Plant Height (in)	1	280	47.8	11	140	31.7	7	70	51.3	11	140	28.8
Leaf Area Index (LAI-2000)	1	280	2.42	10	70	1.33	1	280	2.66	3	0	1.12
Leaf Chlorophyll (SPAD meter)	1	280	51.4	5	0	41.1	1	280	53.7	5	0	37.9
NDVI (CropSCAN)	1	280	0.873	10	70	0.719	7	70	0.885	11	140	0.664
CI (CropSCAN)	1	280	2.65	10	70	1.51	7	70	2.9	11	140	1.35

	July 2, 2010											
	Highest Mean			Lowest Mean			Max			Min		
	Plot#	N	Value	Plot#	N	Value	Plot#	N	Value	Plot#	N	Value
Plant Height (in)	7	70	73.3	3	0	56.9	7	70	82.3	3	0	47.8
Leaf Area Index (LAI-2000)	1	280	3.22	3	0	2.1	1	280	3.36	3	0	1.71
Leaf Chlorophyll (SPAD meter)	1	280	53.5	5	0	38.3	7	70	54.9	5	0	34.6
NDVI (CropSCAN)	1	280	0.91	11	140	0.797	1	280	0.917	11	140	0.728
CI (CropSCAN)	1	280	3.21	12	0	1.75	1	280	3.51	11	140	1.5

	July 17, 2010											
	Highest Mean			Lowest Mean			Max			Min		
	Plot#	N	Value	Plot#	N	Value	Plot#	N	Value	Plot#	N	Value
Plant Height (in)	1	280	93.1	3	0	71.3	1	280	95	3	0	66.5
Leaf Area Index (LAI-2000)	1	280	3.8	3	0	2.71	6	140	3.97	3	0	2.35
Leaf Chlorophyll (SPAD meter)	1	280	53.3	3	0	39.4	1	280	55.4	3	0	36.7
NDVI (CropSCAN)	1	280	0.902	3	0	0.859	2	70	0.906	9	140	0.843
CI (CropSCAN)	1	280	2.98	3	0	1.77	1	280	3.24	5	0	1.59
NDVI (SpecTIR)	6	140	0.814	3	0	0.779	6	140	0.835	6	140	0.69
CI (SpecTIR)	6	140	2.83	3	0	2.07	6	140	1.77	3	0	1.63

Figure 3. Summary tables showing where the highest and lowest values and plot averages, maximum, and minimum values occurred on each date. N=Nitrogen treatment (kg N/ha).

Cluster and Outlier Analysis (Anselin Local Moran's I) corroborated the summary results, identifying clusters of high values (COType=HH, LMI Z>1.96) primarily in Plot 1 (280 kg N/ha) and low values (COType=LL, LMI Z>1.96) in all 3 no-treatment plots.

Coefficients of determination showed that leaf chlorophyll (SPAD), leaf area index, and plant height correlated more highly with RECI than with NDVI. Leaf chlorophyll was expected to show high positive correlations with RECI. Results showed relatively high positive correlations whose coefficients increased as plants reached maturity: June 23 $r^2=0.448$, July 2 $r^2=0.546$, July 17 $r^2=0.695$. Correlations between NDVI and leaf chlorophyll were much lower: $r^2<2.4$. Therefore RECI was shown to be a better determiner of chlorophyll content than NDVI and would likely be preferred for assessing N deficiency from remote sensing data.

Correlations were drawn between each parameter and crop yield (grain weight) to see if yield could be predicted by any one variable over another. RECI won out both July 2 ($r^2=0.401$) and July 17 ($r^2=0.512$) appearing again to be the preferred productivity measure. (See Figure 5.) The relatively low yield coefficients of determination (none above $r^2=0.512$) can be attributed to drought stress experienced during the latter part of the growing season beginning around mid-July just before ears started to develop. The field is non-irrigated and the experiment did not include a soil moisture component to quantify natural variability. Parts of the field that dry more rapidly exhibited greater stress causing uneven yield distributions.

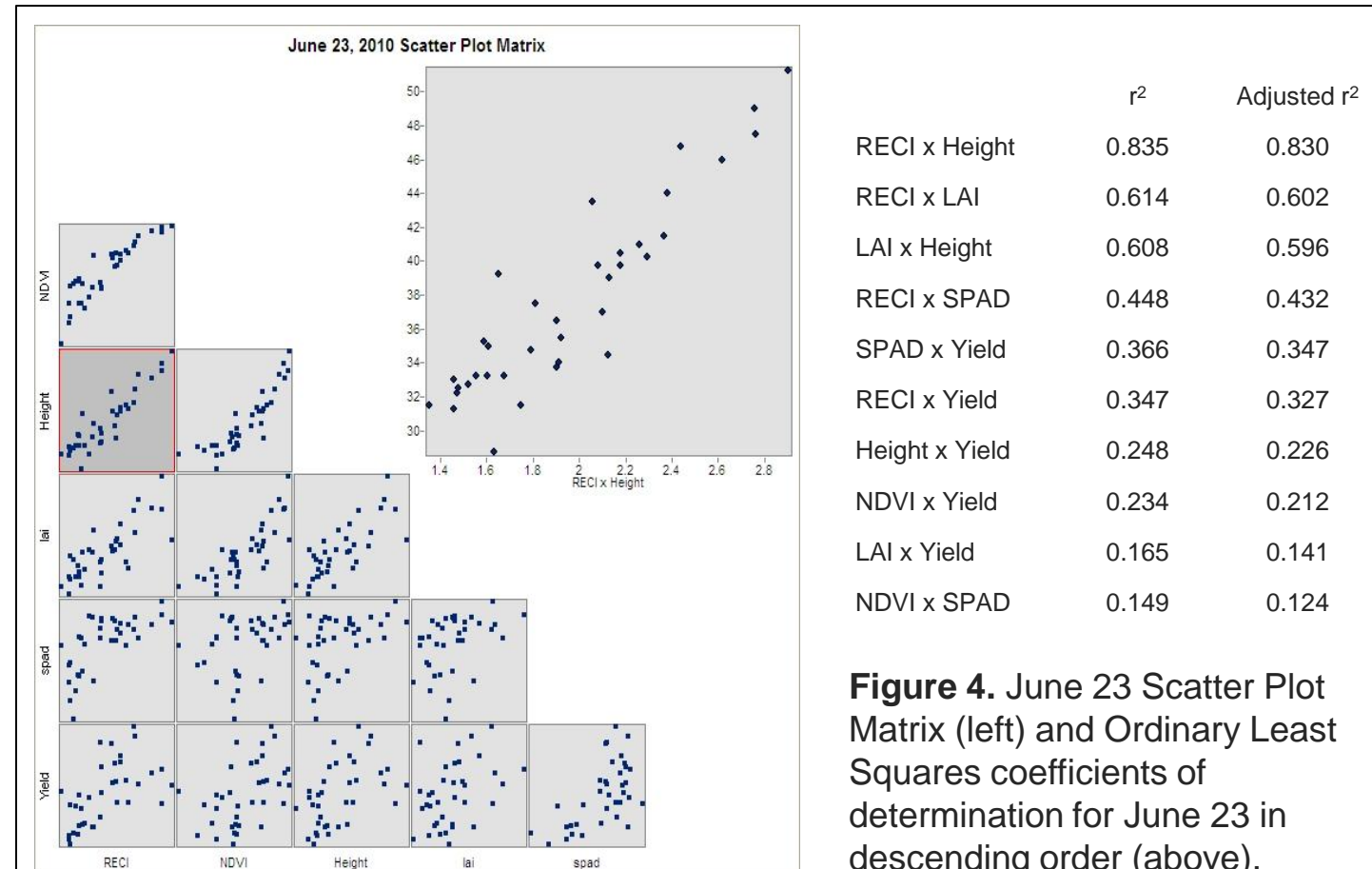


Figure 4. June 23 Scatter Plot Matrix (left) and Ordinary Least Squares coefficients of determination for June 23 in descending order (above).

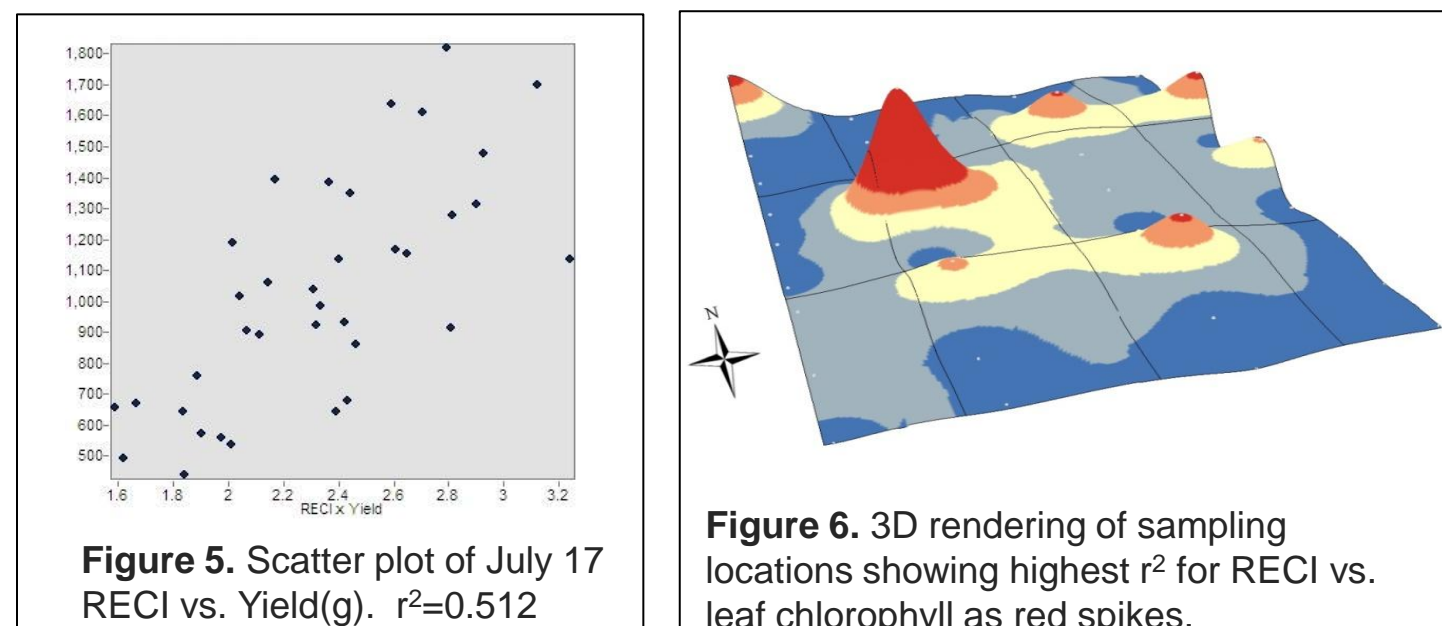


Figure 5. Scatter plot of July 17 RECI vs. Yield(g). $r^2=0.512$

Acknowledgement

Data and OPE3 plan: Andrew Russ, Craig Daughtry, & Tim Gish, USDA-ARS-HRSL.

References

Gitelson A., Keydan, G., Merzlyak, M. 2006. Three-band model for noninvasive estimation of chlorophyll, carotenoids, and anthocyanin contents in higher plant leaves. Geophysical Research Letters 33:L11402.

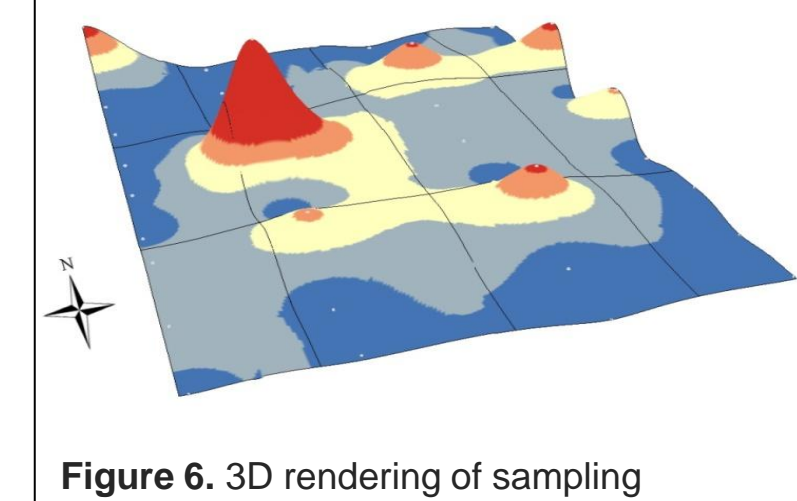


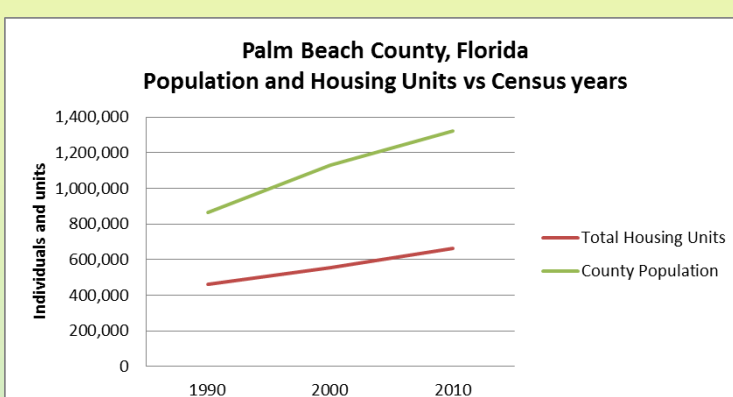
Figure 6. 3D rendering of sampling locations showing highest r^2 for RECI vs. leaf chlorophyll as red spikes.

Abstract

As population increases in an area, the demand for housing may increase. In meeting this demand, cities and counties must balance the need to preserve open spaces, preserves, and agriculture against the pressures to expand the housing stock by developing land. Palm Beach County, Florida, has experienced a 50% population increase and 20% increase in housing units over the past 20 years. How did the land use – land cover of the County change to meet the demand?

Introduction

Palm Beach County, Florida, is the largest county in the state with an area of about 2,400 square miles. Of this area, about 17% is water, and a significant portion of the land is dedicated to agriculture and preservation. As the graph below shows, the population and housing units in the County have increased over time.



In order to manage the land use, the County has zoning regulations that apply to some, but not all of the land – some cities within the County manage their own land use. Given the current land uses and desire to maintain preserve areas, the County should be concerned if LULC changed from preserve to developed uses. Satellite imagery can be used to evaluate the degree to which LULC has changed over time.

Methodology & Data Processing

To evaluate the LULC change over the study period, I selected LANDSAT scenes from October 1990 and January 2011 for comparison. These scenes had the best available combination of temporal consistency and low cloud cover. The methodology was as follows:

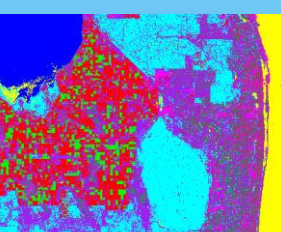
Step 1: Calibrate and mosaic scenes P15/R41 and P15/R42 for 1990 and 2011.



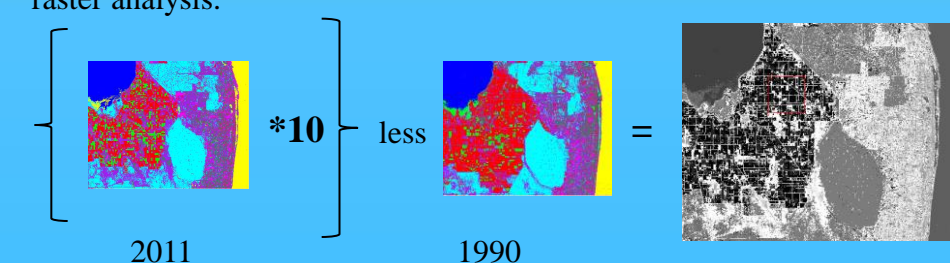
Step 2: Subset the scenes with a shapefile of Palm Beach County obtained from the County GIS data library.



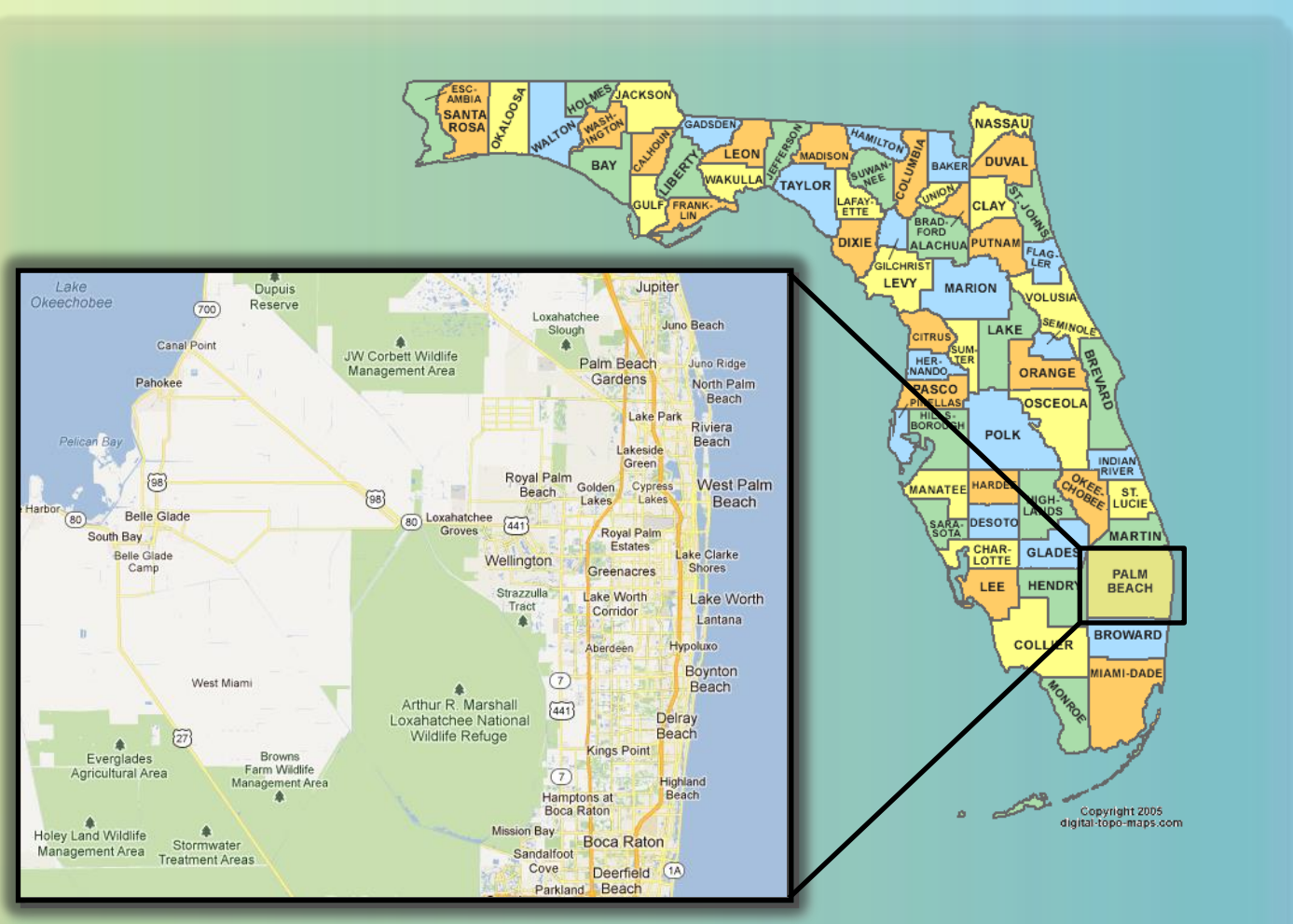
Step 3. Determine ROIs based on the County LULC zoning (and a ground truth ROI) and conduct a supervised classification of the data subset.



Step 4. Use Band math to facilitate LULC change detection and send the resulting image to ESRI ArcMap for raster analysis.



Chris Smith (GEOG652 – Winter 2011)



Classification quality

Before using the classification results for analysis, I developed a confusion matrix for the 1990 and 2011 results which showed an acceptable quality for the features under analysis.

ROI	1990		2011	
	Accuracy		Accuracy	
	Producers	Users	Producers	Users
Agriculture_growing	87.8	93.8	99.5	99.1
Agriculture_fallow	84.5	85.8	58.7	98.4
Lake	98.0	99.9	88.9	97.9
Ocean	99.7	99.8	99.8	99.6
Preserve	88.5	98.0	93.3	97.5
Urban_Commercial	79.8	49.0	80.4	64.3
Residential_High_Density	69.0	71.3	52.2	94.4
Residential_Medium_Density	53.6	79.3	38.7	49.8
Residential_Low_Density	77.2	50.1	84.2	35.9

Analysis

In order to use the band math results, I developed the following chart to determine how to judge what changed and what types of change were most critical to examine. In order to preserve open space and wetlands, you would want to avoid developing preserve land. A common feature of new developments is a series of lakes to handle the runoff from rain, so this would be another indicator of potential and actual development. The table below shows red for LULC changes from preserve to development and yellow (less concern, but worth examining) for developing agricultural land for residential or commercial purposes.

The 1990 LULC was...	...and the 2011 LULC cover is now								
	Agriculture growing	Agriculture fallow	Lake	Ocean	Preserve	Urban or Commercial	Residential High Density	Residential Medium Density	Residential Low Density
Agriculture_growing	9	19	29	39	49	59	69	79	89
Agriculture_fallow	8	18	28	38	48	58	68	78	88
Lake	7	17	27	37	47	57	67	77	87
Ocean	6	16	26	36	46	56	66	76	86
Preserve	5	15	25	35	45	55	65	75	85
Urban_Commercial	4	14	24	34	44	54	64	74	84
Residential_High_Density	3	13	23	33	43	53	63	73	83
Residential_Medium_Density	2	12	22	32	42	52	62	72	82
Residential_Low_Density	1	11	21	31	41	51	61	71	81

I then applied these types of change to the raster image using a tabular join function to produce an image for further analysis. This analysis consisted of looking at areas in red, comparing the land use codes and looking a high resolution image to see the actual conditions on the ground. A selection of the results is shown on the right.

Possible concern
No change
Area of concern
No concern

Results

The image below shows the result of applying the change categories to the differenced classification data. The areas highlighted show where the process did and did not work to identify areas that were preserve in 1990 and developed in 2011.



Discussion & Conclusions

Images #1 and #2 above show where this approach to LULC change did not work. The land was and remains preserve. Images #3 and #4 above show where this approach worked. The land is developed as housing and is zoned as a park preserve. These two cases highlight the practical limits of using LANDSAT data for LULC changes in areas with many LULC types in a fairly compact area.

Analyzing LULC change in urban and suburban areas using 30m resolution LANDSAT data is adequate for establishing areas for further investigation of possible land use or zoning violations, but for definitively determining that a particular parcel of land is being properly used, you would need 15m or better resolution imagery combined with hyper-spectral images to better differentiate between the various LULC types that are in close proximity in a combination urban/suburban/rural scene like the one used for this analysis.

In this case, it appears that the development in Palm Beach County to accommodate the increased population was done almost exclusively by increasing the density of already developed areas and using parts of the County designated for development and not by building on areas set aside for preservation.

LiDAR Applications in Slope Failure

J. Hoon-Starr

Abstract

Statewide Light Detection and Ranging (LiDAR) data is becoming more readily available for environmental groups and companies to use free of charge for monitoring and planning. Over four million miles of highways exist in the continental US and a large portion in the north and west pass through extensive mountainous terrain. The purpose of this research is to determine a simple and cost effective method to determine areas with steep non-vegetated slopes which pose risk of slope collapse infrastructure



Figure 1 - The study area here can be seen to include past slope failures, and rough bare and vegetation covered slopes

Introduction

LiDAR is an optical remote sensing technology that returns referenced point cloud altimetry data as well as intensity data that can determine surface structure, vegetation, and composition. States are completing extensive LiDAR surveys and providing the data to users free of charge with increasing regularity. Slope stability can be estimated with high spatial resolution without additional data or ground measurements.

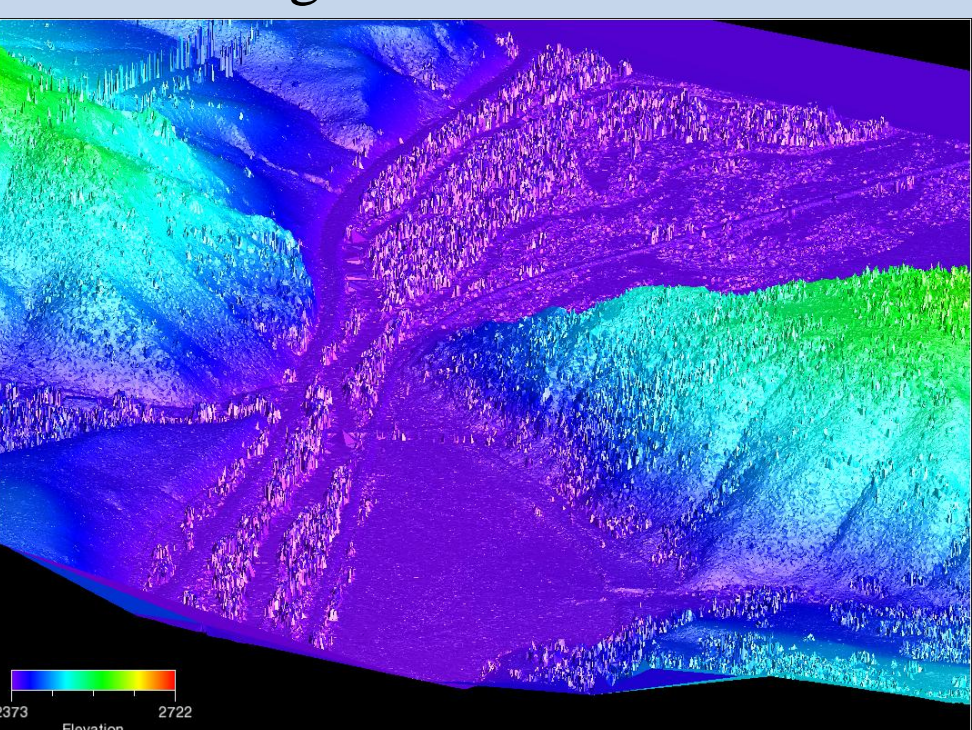


Figure 2 - This study area displays a visual representation of the LiDAR data which is color coded by elevation.

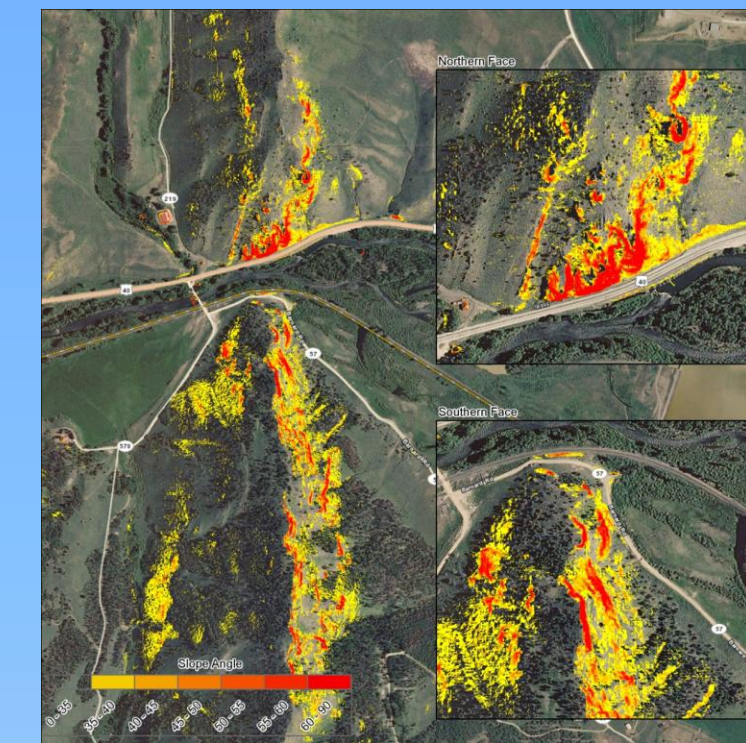
Study Area, Data and Tools

The observation area is a segment of the Rocky Mountains near Rt. 40 in Colorado

LiDAR provided by the United States Geological Survey and accessed through the Open Topography portal.

Analysis was done with the BCAL LiDAR open source tools provided by the Boise Center Aerospace Laboratory

Figure 3 – Color coded values demonstrate the slope in degrees of the bare earth digital elevation model. Slope angles from 60° to 90° have the highest risk whereas 35° has the lowest



Methodology

The initial intent was to use the point cloud to extract a bare earth DEM which could be used to calculate slope angle. Areas with high slope and no vegetation coverage were to be classified as high risk however the algorithms to determine vegetation density and coverage had extensive difficulty in rough mountainous terrain.

The height and return number of the LiDAR point cloud is analyzed and the algorithm estimates surface structure without vegetation.

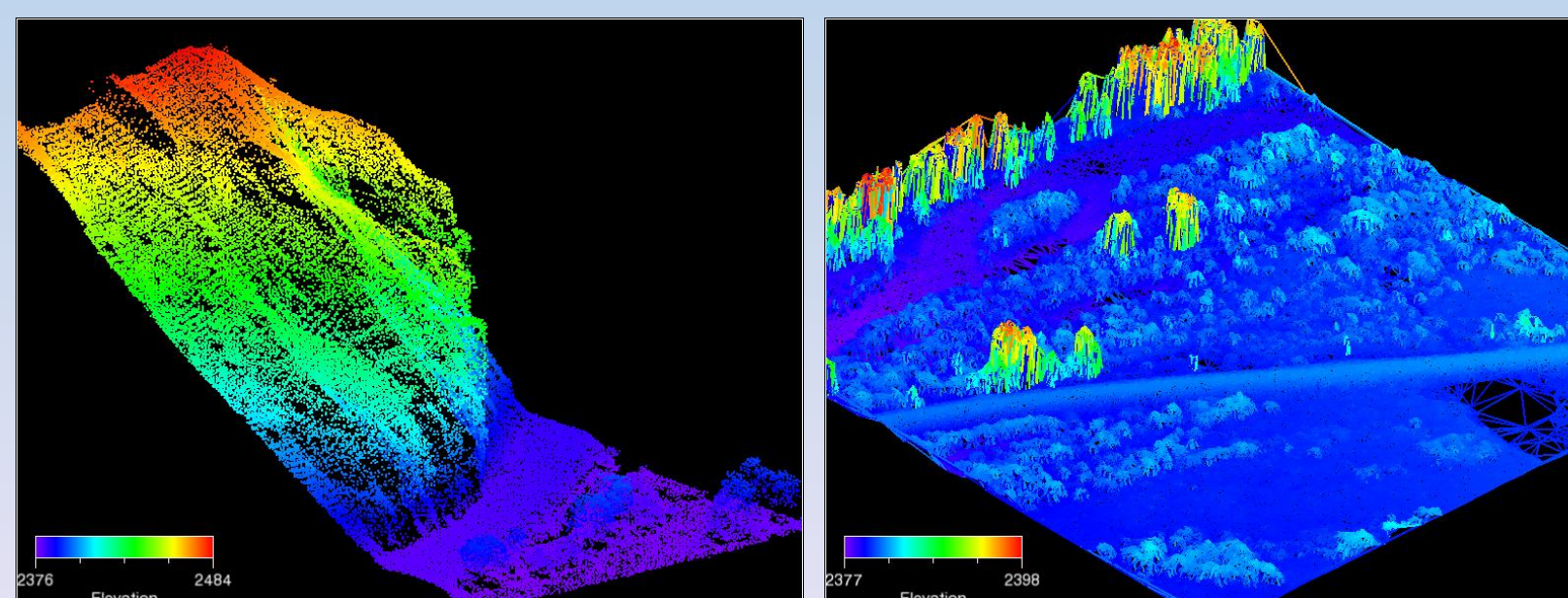


Figure 4 – A 3D representation of the northern rock face shows the high degree of change on the z axis

Figure 5 – Tall vegetation has much higher degree of local roughness than low vegetation or high angle slopes

Results

Weighing vegetation density algorithm using the local roughness of each pixel allows a simple threshold to separate tall vegetation from low lying vegetation and high angle surfaces

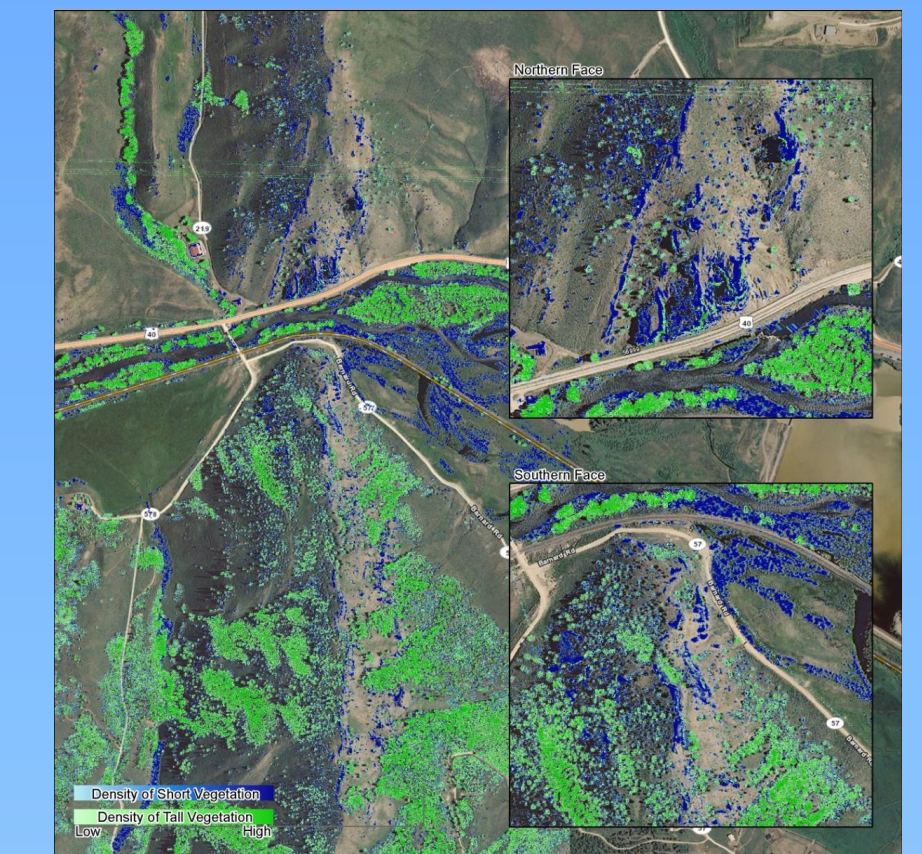


Figure 6 - Green covers tall stands, blue covers short as well as some of the slope features

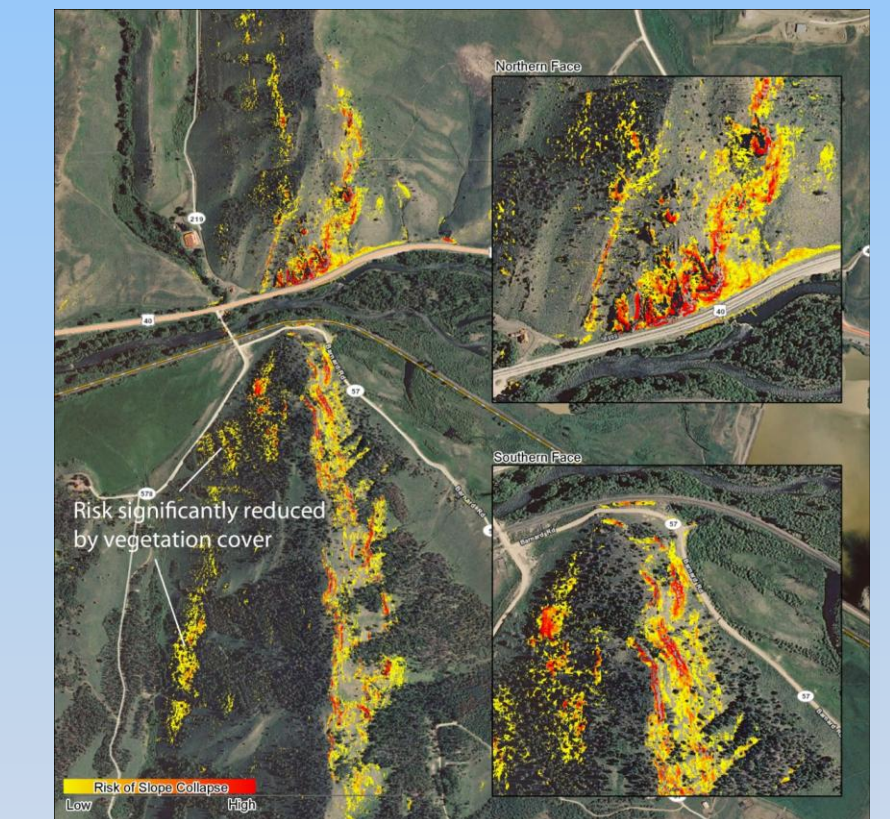


Figure 7 - Removing all high risk slope areas within 1 meter of tall vegetation areas gives us a map of high angle bare slopes which have the highest risk of collapse

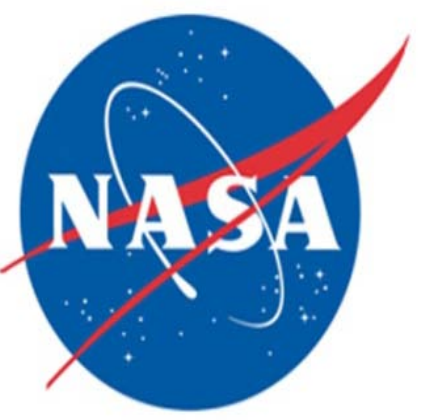
Conclusions

Steep bare slopes can be determined at high spatial resolutions using publicly available LiDAR data which could automatically determine areas of possible slope collapse.

References

- Erismann, T. H., & Abele, G. (2001). *Dynamics of rockslides and rockfalls*. Berlin: Springer.
- Smart, C. L. (2009). *Slope Failure*. Retrieved Feb 10, 2011, from Kean University:
<http://www.kean.edu/~csmart/Observing/12.%20Slope%20failure%20and%20landslides.pdf>

Using the MODIS Active Fire Product to Observe Changes in Spatial Patterns of Fire Regimes in Tropical, Sub-Tropical, and Temperate Biomes



Michael L. Humber
University of Maryland

Abstract

The availability of daily, global data at moderate resolution has greatly increased the capacity to monitor large scale trends over the past decade. By employing MODIS Active Fire Climate Modeling Grid (MOD14 CMG) data, it is possible to identify large scale, spatiotemporal patterns in wildfires across a variety of biomes.

While all biomes have a clear pattern with regard to the fire regime, this pattern varies from region to region based on the geographical north/south extent of the biome.

Introduction

Wildfires are catastrophic natural events which occur with a high degree of regularity around the world. Although wildfire frequency is linked to anthropogenic factors, such as population density and fire suppression leading to increased fuel loading, the spread of fires and their intensities are influenced more by microclimatic and ecological factors which come as a result of non-anthropogenic processes (Syphard, et al., 2007; Ray et al., 2005). Because fires are largely influenced by non-human factors, it seems appropriate to analyze the associated patterns based on these factors.

This research will seek to determine if there is a significant amount of spatial variability in patterns of wildfires in various ecoregions which, presumably, comes as a result of climatic factors associated seasonality. To this end, the aim of this research is to answer the question, "How does seasonality influence patterns in global fire regimes?"

Study Area

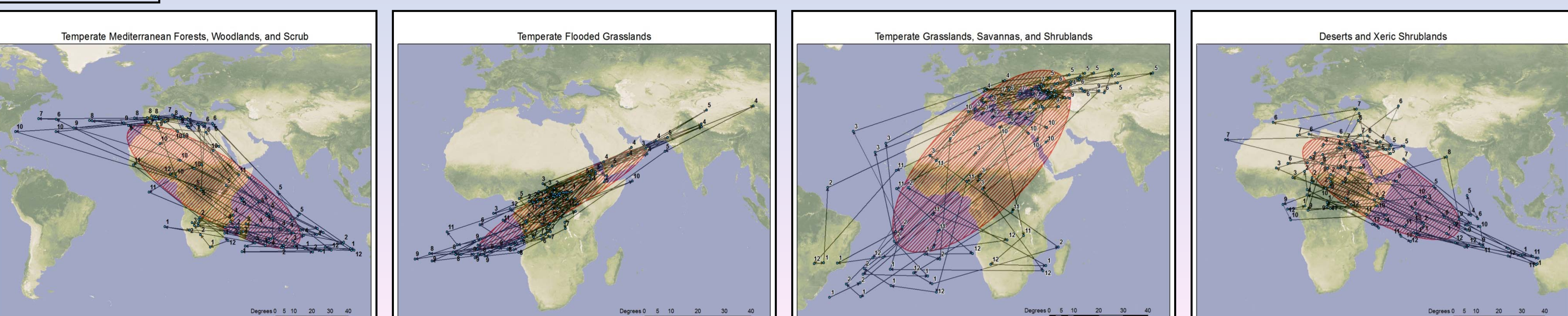
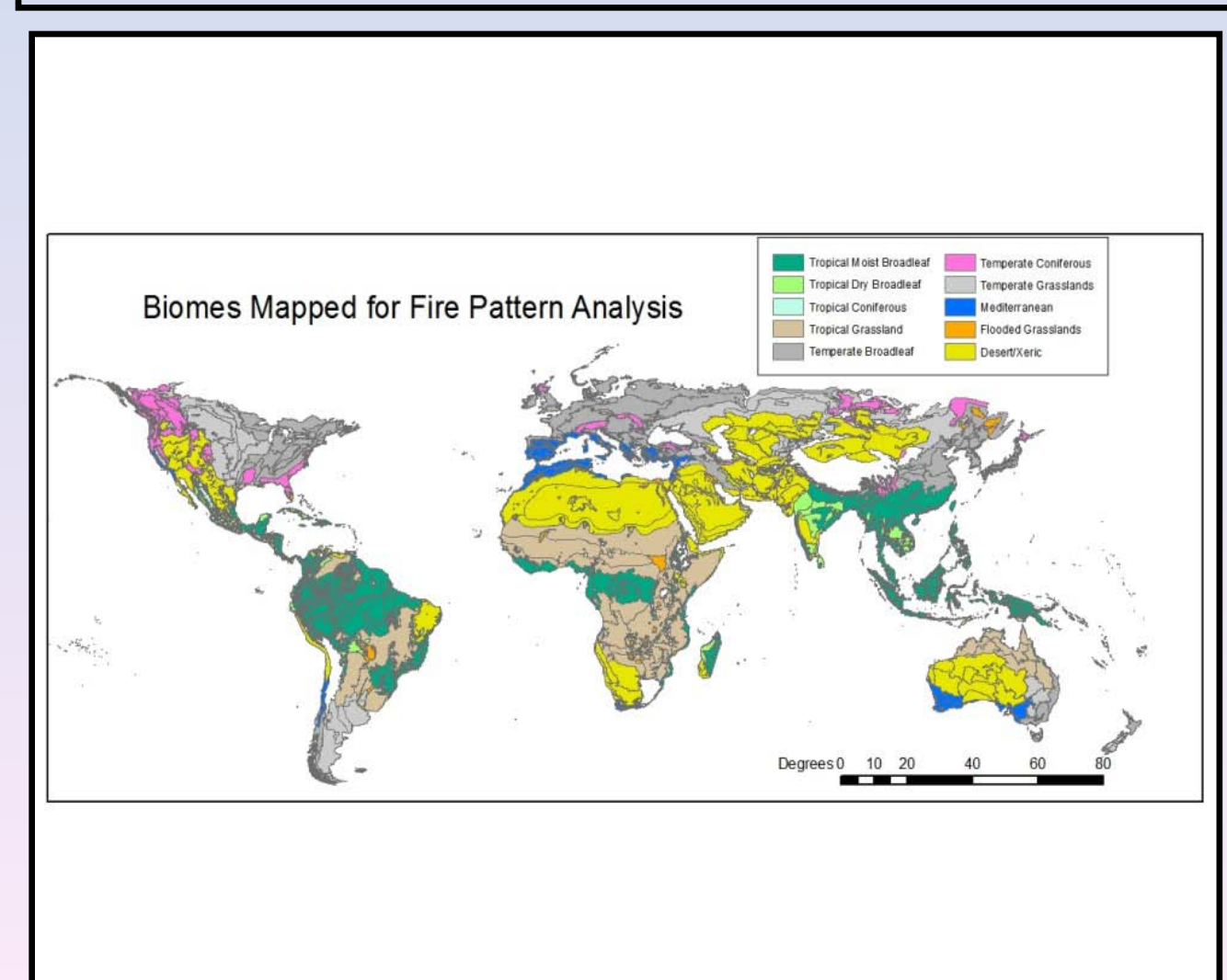
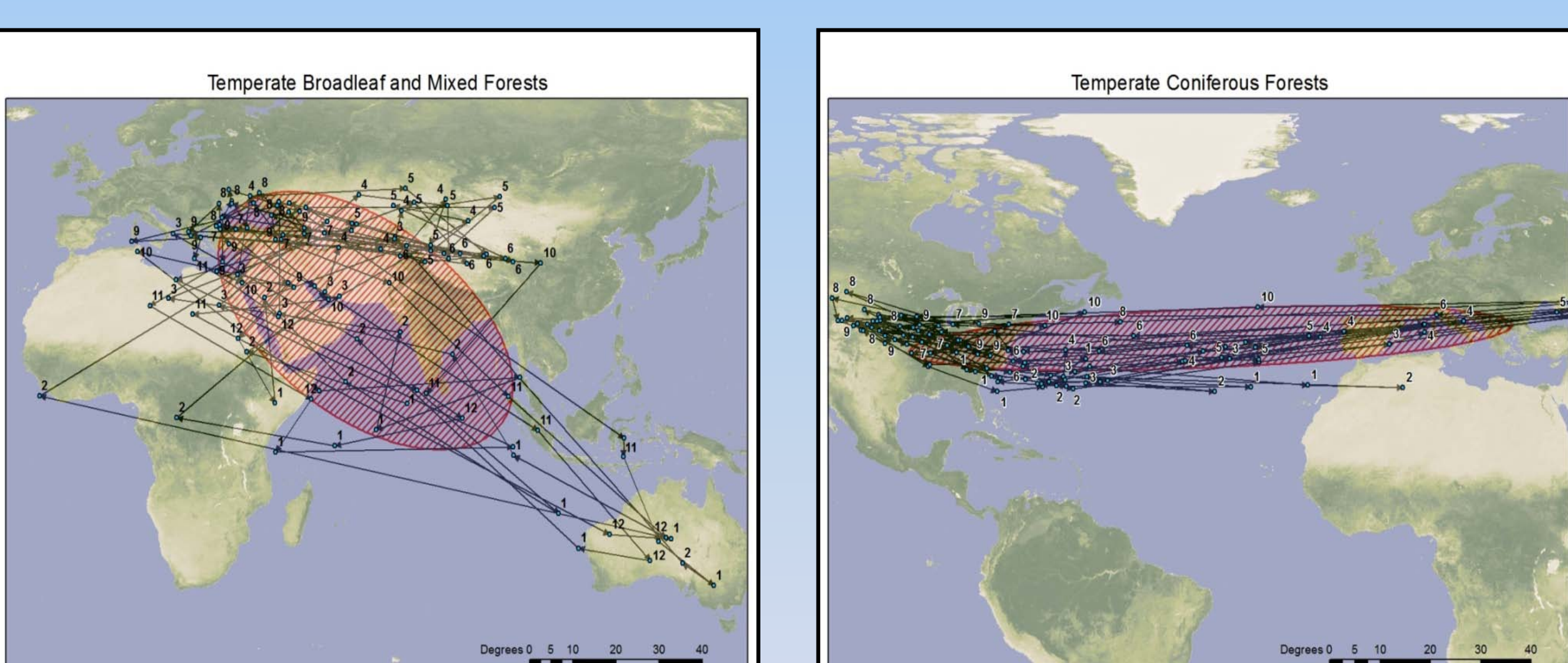
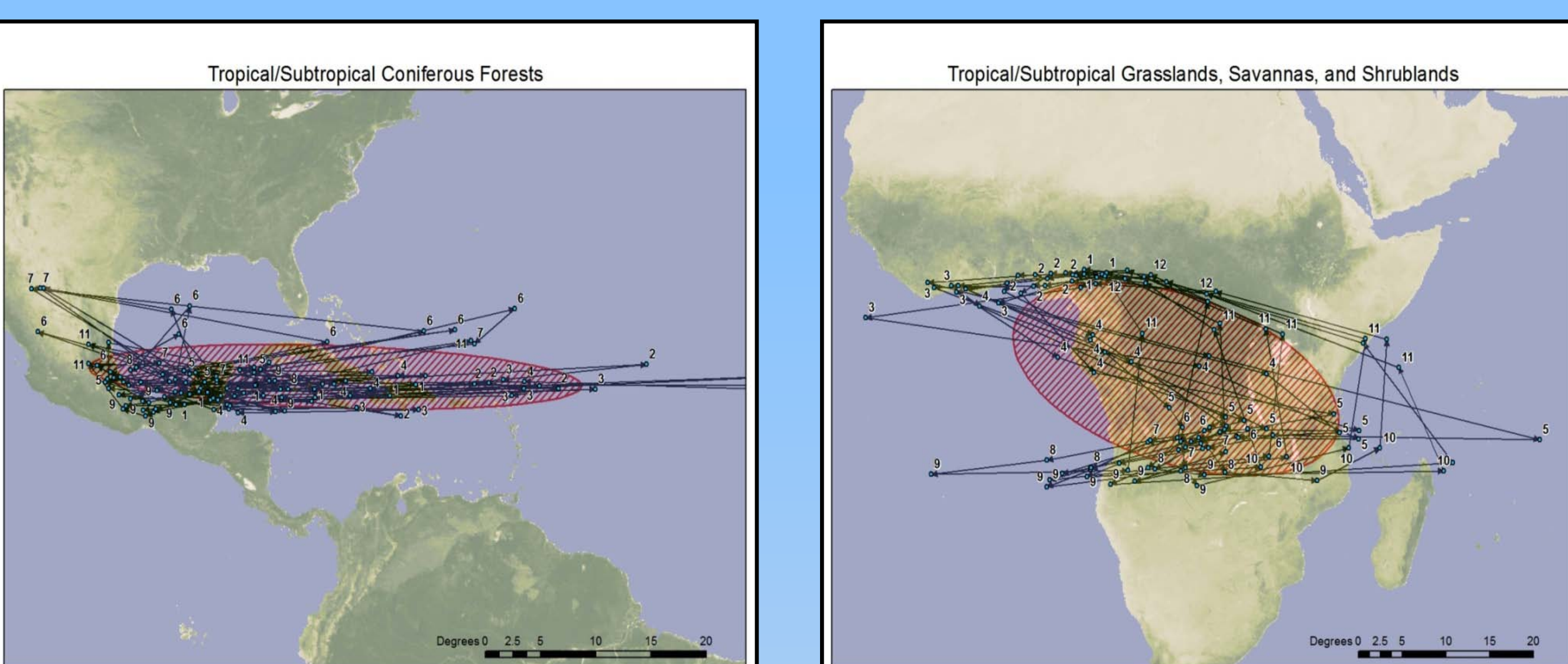
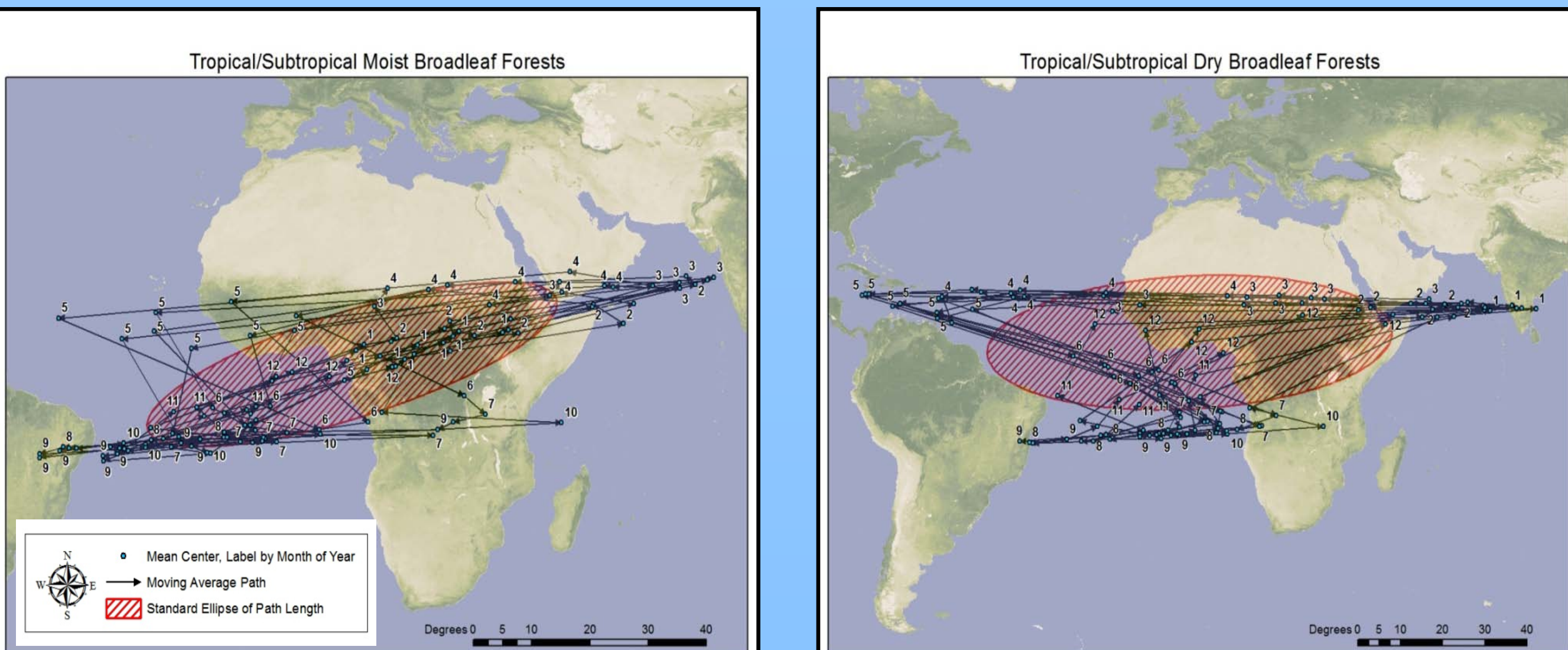
This research was conducted on a global/regional scale, utilizing the Terrestrial Ecosystems map adopted by the World Wildlife Fund (WWF). Under the Terrestrial Ecosystems classification system, fifteen distinct biomes are adopted which represent the entirety of the planet's land mass. Of these fifteen, ten of these ecosystems were selected due to the quality of data available:

- Tropical and Subtropical: Moist Broadleaf Forests; Dry Broadleaf Forests; Coniferous Forests; Grasslands, Savannas, and Shrublands
- Temperate and Non-tropical, Non-desert: Broadleaf and Mixed Forests; Coniferous Forests; Grasslands, Savannas, and Shrublands; Mediterranean Forests, Woodlands, and Scrub; Flooded grasslands
- Desert and Tundra: Deserts and Xeric Shrublands

Data

This research relies heavily upon the MODIS Active Fire Climate Modeling Grid (MOD14 CMG) product, which contains monthly composites of active fire detections corrected for cloud cover and spatial distortion at 0.5x0.5 degree resolution. These data are available from November 2000 to August 2011. The ten year period from January 2001 to December 2010 was selected for this analysis. The CMG data are available as a .hdf raster format from the University of Maryland Fire Information Resource Management site (www.maps.geog.umd.edu/firms)

As mentioned, the Terrestrial Ecosystems dataset, available from the WWF, was used to define the boundaries of the biomes selected.



Methods

To represent the pattern of fires within each biome, the per-month mean center of all fires within each biome was calculated and weighted by the number of fires per cell. These data were then aggregated to create a single file for each biome containing 120 mean center calculations representing the 10 year study period.

From the mean center calculations, it is possible to show the "path" of the average, which ultimately represents the oscillation of the fire regime between 2001 and 2010. Because the time interval between each sample is constant (one month), each line segment represents the net difference in mean center between two months and the length of each segment therefore is indicative of its rate of change. Thus, the line segments, when weighted by length, produce a standard deviational ellipse with a major axis which shows the direction of most rapid change.

Results and Discussion

Fire patterns vary most significantly as a function of latitude and the north/south extent of the study area. While all biomes show a cyclical pattern of mean fire centers, tropical biomes follow a much stricter pattern than their temperate and desert counterparts. Additionally, the southern portion of the seasonal oscillation in tropical and subtropical biomes corresponds to the months surrounding September while the northern portions of the oscillation correspond to months nearer to March. Temperate biomes and deserts, on the other hand, show that fires are more prevalent in the north during July and its surrounding months (Summer in the northern hemisphere, Winter in the southern), with the mean center migrating south during December and its surrounding months (Summer in the South, Winter in the North).

While the pattern shown by temperate biomes is explained by the seasonal difference caused by insolation changes as a result of the tilt of the Earth's axis, the pattern found in the tropical is characterized by East/West changes in mean center, as illustrated by the standard ellipses. Due to the consistency of the patterns in tropical regions, it is possible that the fire regime is governed by the wet-dry season effect caused by the Intertropical Convergence Zone rather than insolation disparities.

Acknowledgements

The author would like to thank the MODIS Fire Team and Alexandra Moulden for providing the data used in this research.

References

- Dwyer, E., J. Pereira, J. Gregoire, C. DaCamara, (2000) Characterization of the spatio-temporal patterns of global fire using satellite imagery for the period April 1992 to March 1993, *Journal of Biogeography*, 27(1), p.57-69
- Syphard, A.D., V.C. Radeloff, J.E. Keeley, T.J. Hawbaker, M.K. Clayton, S.I. Steward, R.B. Hammer (2007) Human Influence on California Fire Regimes, *Ecological Applications*, 17(5), p. 1388-1402
- Thonicke, K., S. Venevsky, S. Stich, W. Cramer (2001) The role of fire disturbance for global vegetation dynamics: coupling fire into a Dynamic Global Vegetation Model, *Global Ecology & Biogeography*, 10, p.661-677